AN EVALUATION OF THE MEASURING TECHNIQUES USED IN HIGH STRAIN RATE TESTING OF MATERIALS

by

SAYEEDUDDIN SYED

M. Sc., Osmania University, 1964
B. S., Kansas State University, 1966

A MASTER'S REPORT

submitted in partial fulfillment of the

requirements for the degree

MASTER OF SCIENCE

Department of Mechanical Engineering

KANSAS STATE UNIVERSITY
Manhattan, Kansas

1968

Approved by:

Major Professor

TABLE OF CONTENTS

NOMENCLATURE

A = Area (sq. in.)

D = Diameter (in.)

E = Modulus of elasticity (p.s.i.)

W = Energy (in. lb.)

F = Force (lb.)

g = Acceleration due to gravity (in./sec./sec.)

h = Wall thickness of cylinder (in.)

L = Gage length (in.)

m = Mass (lb. m.)

P = Pressure (p.s.i.)

R = Radius (in.)

t = Time (sec.)

V = Velocity (in./sec.)

ΔL = Increase in length (in.)

ϵ = Strain (in./in.)

$\dot{\epsilon}$ = Strain rate ($sec.^{-1}$)(in./in./sec.)

σ = Stress (p.s.i.)

ρ = Density (lb./cu.in.)

INTRODUCTION

Obtaining valid data that shows the dependence of mechanical properties of materials on strain rate is a difficult task. Certain investigators have found that some materials are weaker at high speed; others that materials are stronger at high speed. For this type of research, tensile impact tests have been performed by many investigators using pendulum machines, rotating disc impact machines, explosive impact machines, or other types. The strain rates obtained by these methods range from 10^{-4} in/in/sec (sec^{-1}) to 25,000 in/in/sec. In this report are described twelve experiments performed by different workers. Different techniques of measuring stress, strain, and strain rates are given. The results are given separately for each experiment, and finally the correlation of these results is made.

Shepler (1)* used an explosive tensile loading test to obtain strain rates near 25,000 sec^{-1}. Hoge (2) performed his experiments on a Dynapak metal working machine which utilizes the power from high pressure nitrogen. Anderson (3) also performed experiments on a machine in which nitrogen is used as a power source. A rotating disc impact testing machine was used by Clark (4) to obtain high strain rates. Hoge, Clark, and Anderson were able to obtain strain rates of the order of 16 to 150 sec^{-1}. Manjoine and Nadai (5) obtained strain rates up to 900 sec^{-1} by using a rotating disc impact testing machine

---

*Numbers in parenthesis refer to bibliography.

similar to the one used by Clark. Smith (6) performed experiments on pendulum type impact machine to obtain strain rates up to 200 sec^{-1}.

The results obtained from the above mentioned experiments were based mainly on the initial and final measurements. Steidel and Nikerov (7) used a pendulum impact machine, similar to the one used by Smith, but utilized a high-speed camera, with a speed of 7000 frames per second, to obtain the reduction of area as a function of time. They obtained strain rates up to 100 sec^{-1}. Steidel and Austin obtained strain rates near 17,000 sec^{-1} by means of an explosive tensile testing machine, and the instantaneous values of diameter and velocity were obtained by means of a high-speed camera, about 3 million frames per second. The results given in this report are for specimens of copper, steel, and aluminum.

The above mentioned tests were performed on solid rod specimens. In the following experiments, tubular specimens were used. Randall and Ginsburgh (9) used a shock tube testing machine and obtained strain rates around 900 in/in/sec. Clark and Duwez (10) and Noyes (11) used tube impact test fixtures and obtained strain rates of the order of 200 in/in/sec. Strain rates of about 35 in/in/sec were obtained by Hoge by using a modified Dynapak impact machine.

TESTING TECHNIQUES

Solid Rod Specimen

All the specimens used were of the stenderd type as shown in Fig. 1 except the one used by Shepler. His had e curved taper as shown in Fig. 2. Load cells were used to obtain loed as a function of time; these were connected in series with the specimen. In most of the experiments, the load cell was connected to the stationery end of the specimen. Anderson, Steidel and Makerov, and Smith ettached the cell to the end at which the load was applied, moving end. Effect on the results due to the mass forward of the gages on the load cell was ignored. Hoge atteched strain gages directly to the test section of the specimen to compare results with the load cell. Agreement was good.

Shepler used en explosive loaded tensile test to determine the properties of materials under high strain rates; see Fig. 2 and Appendix I for detailed information of the machine. For determining the velocity and displacement, en accelerometer (see Fig. 2) wes fixed to the moving end of the specimen. Strain gages were mounted on the eccelerometer two inches from the front end. Mass forward of these wires ceused a measureble force from which an acceleration-time curve wes obtained. A single integration of the eccelereticn-time curve gave the velocity, end a double integretion gave displecement. A calibretion test was run on the eccelerometer to determine its eccurecy.

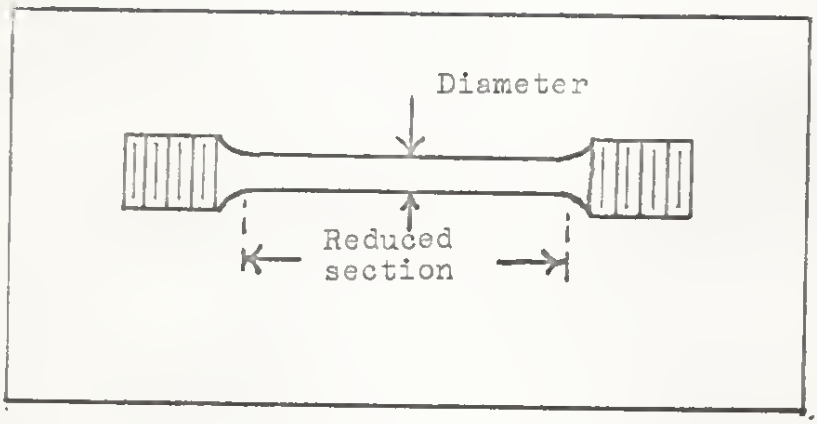

Fig. 1. Test specimen.

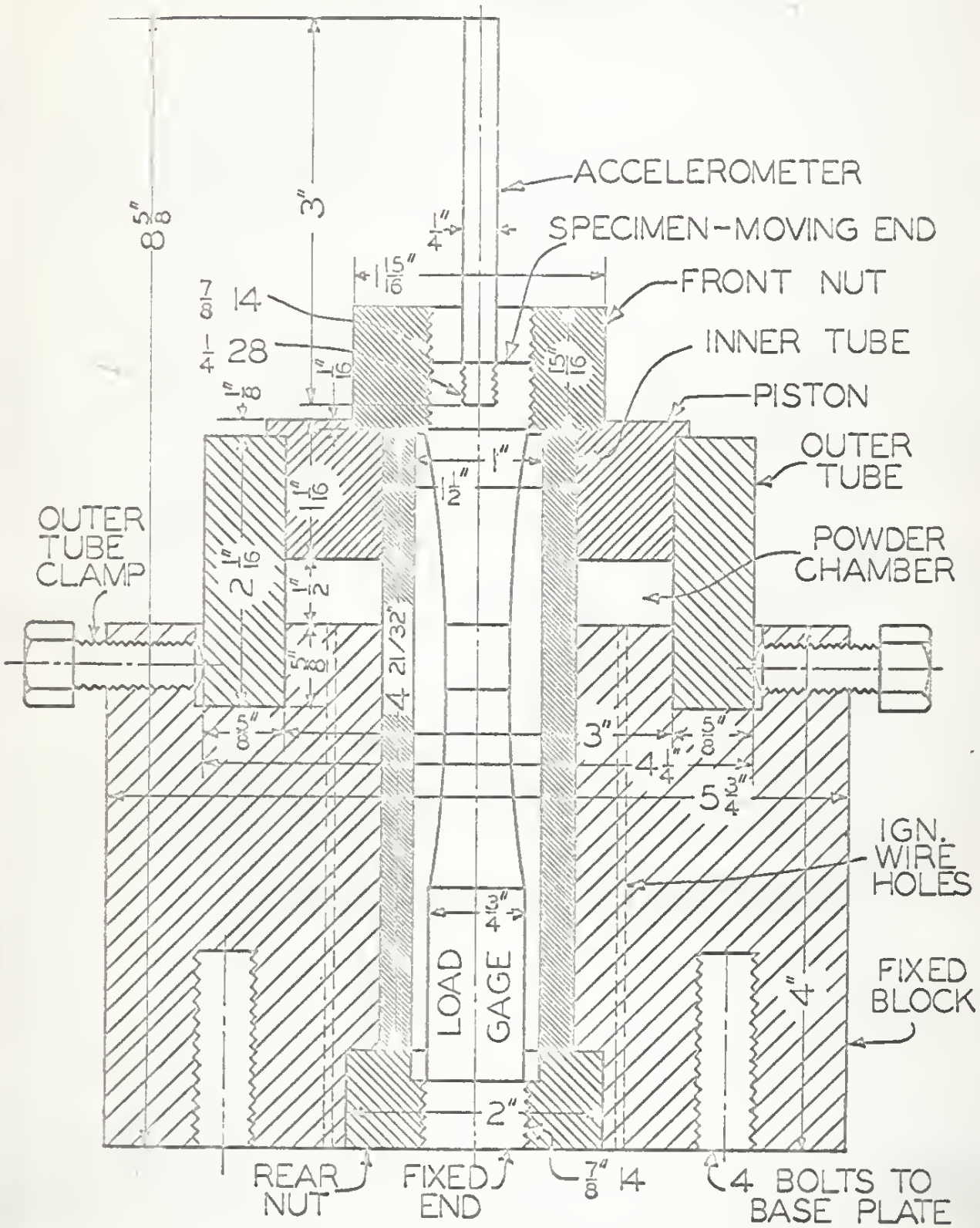

Fig. 2. Testing machine, Shepler.

before applying the load circumferential rings were marked on the specimen. Measurements of the diameter at those rings were made before and after the test and used in calculating true strain. The oscilloscope display of the load cell and accelerometer outputs were recorded on film by means of a rotating drum camera.

Stresses were obtained by dividing the fracture load by the actual area at fracture. Strains were calculated from the change in the diameters of the rings marked on the specimen. The nominal true strain rate at fracture, $\dot{\epsilon}_{fn}$, was calculated as follows.

$$\dot{\epsilon}_{fn} = \frac{k \ \ell n \ A_o/A_f}{t_p}$$

where A_o and A_f are initial and final areas,

t_p is the time from yield to fracture,

k is the factor of proportionality, ratio between the velocity at fracture to the average velocity from yield to fracture, $k = V_f/V_p$.

Shepler defined average true strain rate from yield to fracture as $\dot{\epsilon}_p = \frac{\ell n \ A_o/A_f}{t_p}$, and the nominal true strain rate at fracture as

$$\dot{\epsilon}_{fn} = \dot{\epsilon}_p \times \frac{\dot{\epsilon}_{fn}}{\dot{\epsilon}_p} .$$

Average true strain rate from yield to fracture, $\dot{\epsilon}_p$, could be calculated from the experimental results. Shepler assumed the

ratio $\dot{e}_n/\dot{e}_p$ to be the same as the factor of proportionality, k, in determining the nominal true strain rate.

Hoge used the Dynapak metal working machine, Fig. 3 and Appendix I. Ultimate strength was calculated by using the original area; fractured area was used to calculate rupture strength.

Strain and strain rates were calculated from the output of a velocity transducer attached to the specimens' threaded ends. The velocity transducer output voltage, e, was integrated by a Tektronix type O preamplifier. The integrated output, e_o, was related to the displacement, ΔL, as follows.

$$e_o = - \frac{1}{RC} \int_0^t e \, dt$$

$$\Delta L = \int_0^t V \, dt = - RC \, e_o/K$$

where V = deformation velocity,

R = resistance,

C = capacitance,

K = conversion constant.

The conversion constant K was obtained directly from the slope of the calibration curve, Fig. 4a, which shows the excellent linearity of the transducer. Strains were obtained by dividing elongations by the original test section length (1.75 inches gage length). Strain rates were obtained from a plot of ΔL as a function of time. Because the transducer was measuring certain displacements which were not occurring in the reduced area

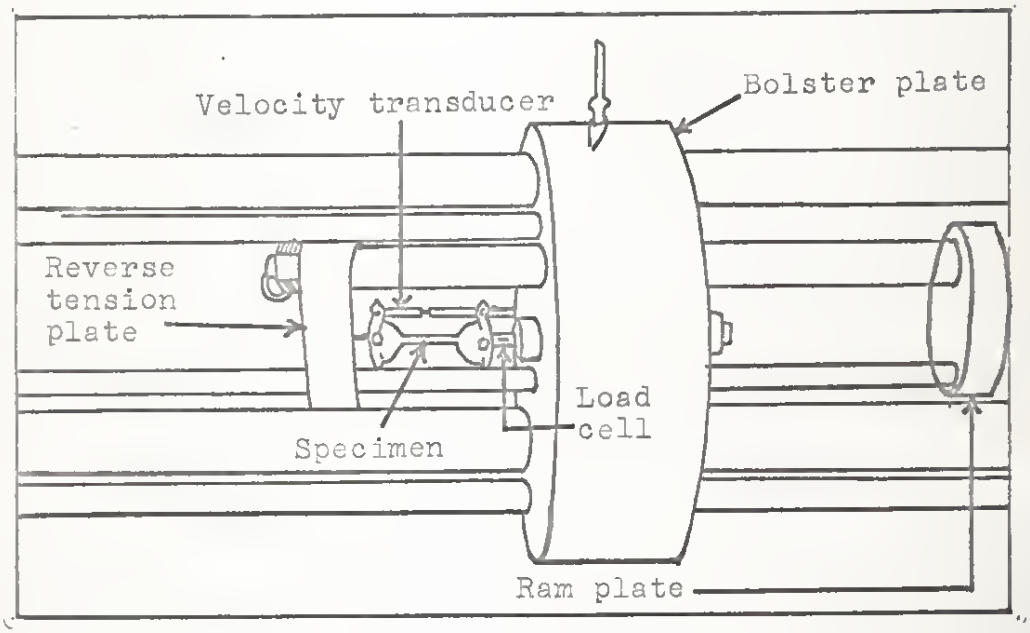

Fig. 3. Dynapak testing machine, Hoge.

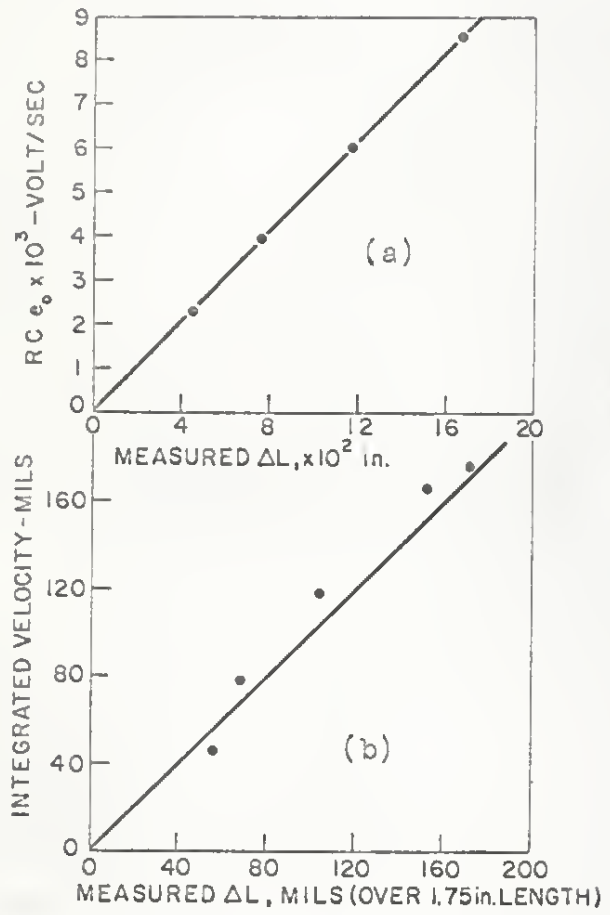

Fig. 4.

a. Velocity transducer calibration curve.

b. Validity curve for the velocity transducer.

section, validity tests were run using a universal testing machine to check the magnitude of errors. Actual displacements were taken between scribe marks defining the reduced area section. Figure 4b compares these displacements with the integrated transducer readings.

Anderson used a tensile test machine which also utilizes high-pressure gas for driving, Fig. 5 and Appendix I, a crosshead (yoke). Travel was measured by means of a linear potentiometer gage attached to the fixed frame, and actuated through a wiper and a rod attached to the moving crosshead. Results on the oscilloscope show that crosshead speed is nearly uniform until the maximum load is reached which indicates that speed is virtually unchanged during general and local extension. The results obtained from the gages mounted at the middle of the specimen over a gage length of 0.25 inch, show that the actual strain increases at a very high rate during localized tension. Because of this, Anderson used the results from strain gages to obtain strain and strain rates.

A rotating disc type impact machine was used by Clark, Fig. 6 and Appendix I. It was found that due to the inertia of the rotating mass, and because of the relatively small energy required to rupture the specimen in tension impact, the velocity of the wheel was effectively constant during fracture.

To obtain the stress-strain curve, the load-time diagram was used. By knowing the peripheral velocity of the wheel, the increase in the length of the specimen could be calculated at any time after the impact; at the same time, for a particular

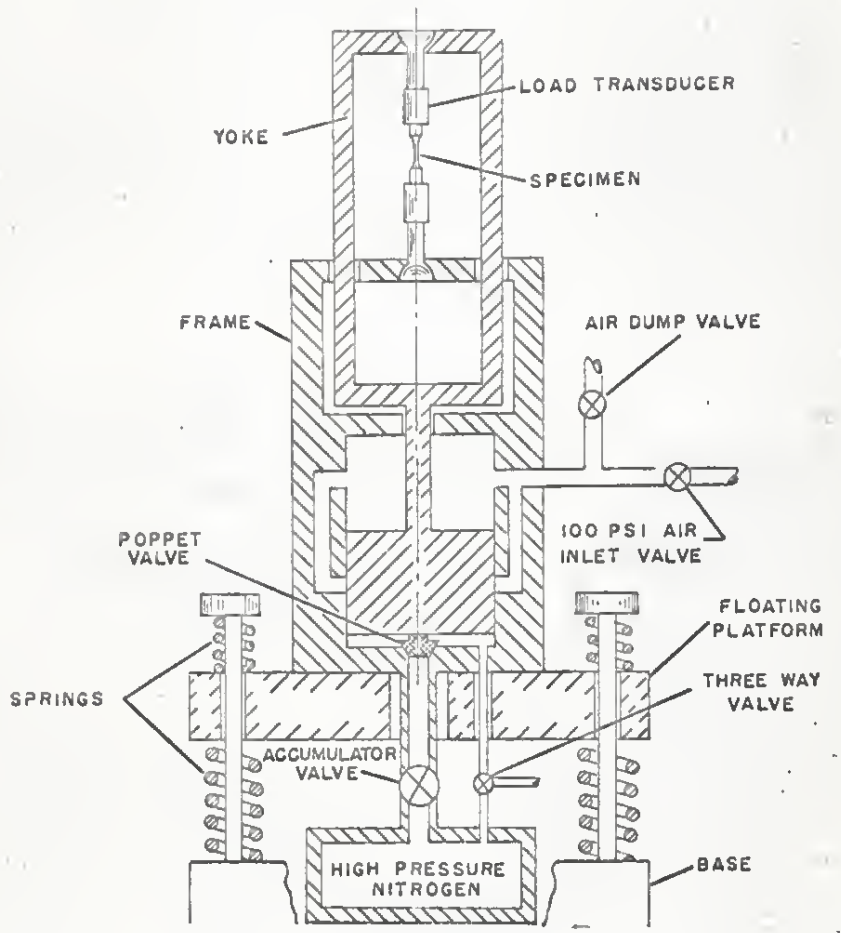

Fig. 5. Tensile tester, Anderson.

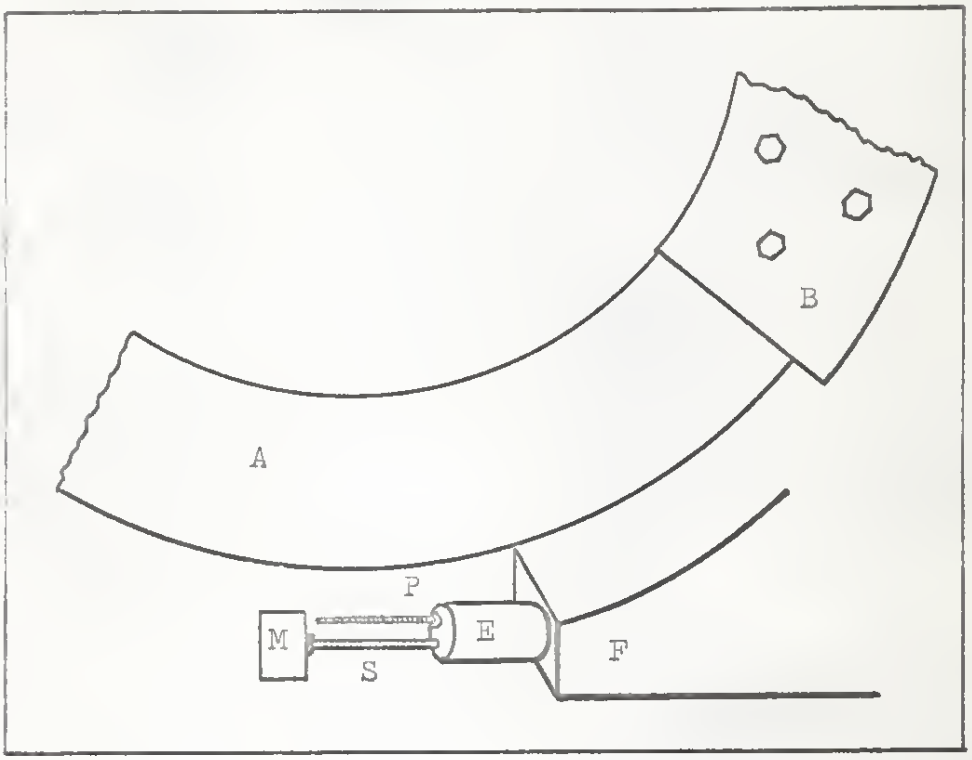

Fig. 6. High-speed tension test machine, Clark.

A = Rotating disc
B = Striking jaws
E = Dynamometer
F = Anvil
M = Tup
P = Extensometer
S = Specimen.

increase of length, the corresponding load could be obtained from the load-time diagram. By knowing the initial area and length of the specimen, stress and strain could be calculated. Using this data strain versus time could be plotted, from which strain rate could be calculated. Points at which yield stress, ultimate stress, and breaking stress occurred, were obtained from the load-time diagram.

The tensile loading machine used by Manjoine and Nadai (Fig. 7) was similar to the one used by Clark. Manjoine and Nadai used a load measuring method which was slightly different from the others, k through o, Fig. 7. The fixed end of the specimen, c, was attached to the force measuring bar. At the upper end of this bar a vertical pin was welded. The upper end of the pin formed a 0.002-inch slit with a fixed pin located above it. A beam of light was projected through the slit onto a photoelectric cell. The force transmitted through the specimen stretches the bar, which, in turn, pulls down the pin, causing a slight increase in the width of the slit. This causes more light to pass through it to the photoelectric cell. The response of the photoelectric cell was calibrated to give the load.

For strain measurement, a second optical system with a photoelectric cell was provided, Fig. 7, d, p, q, and s. The light of a small lamp was converted to a parallel beam of light between two condensing lenses. When the anvil, d, due to the stretching of the test specimen, moves downward, it intercepts the light beam, and the resulting decrease of light causes a

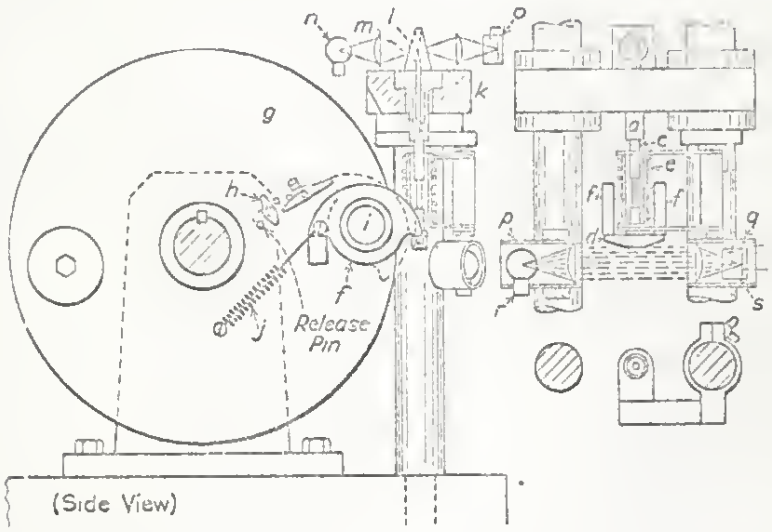

Fig. 7. High-speed tension test machine, Manjoine and Nadai.

a = Force measuring bar
c = Test specimen
d = Anvil
f = Pair of hammers
g = Rotating disc
j = Spring
k = Upper lead
  = Slit
m = Vertical pin
n,r = Light sources
o,s = Photoelectric cells
p,q = Brass tubes.

response of the photoelectric cell which is recorded on an oscilloscope. This gives elongation of the specimen as a function of time. From this strain could be obtained, using the original length of the specimen. Strain rate could be obtained by plotting strain versus time.

Smith used a pendulum type impact machine, as shown in Fig. 8. Two strain gages were mounted on opposite sides of the reduced section to give an accurate indication of initial strain, as well as the yielding behavior. Velocity and displacement of the moving end of the specimen were calculated as follows. During the period from t_o, the time of contact of cross bar and anvil, to fracture of the specimen, the pendulum head is sufficiently near the horizontal to allow its energy to be expressed as

$$E' = E_o' - \int_{t_o}^{t} F\ V\ dt$$

where E' is the pendulum energy at any time t,

E_o' is the pendulum energy at t_o,

F is the load supported by tension specimen

V is the linear velocity of the center of percussion.

This integral can be written in the following finite difference form:

$$E'_{k+1} = E_k' - \bar{F}_{k,k+1}\ V_k(t_{k+1} - t_k)$$

where E_k' is the pendulum energy at $t = t_k$

V is the linear velocity of the center of percussion at t_k,

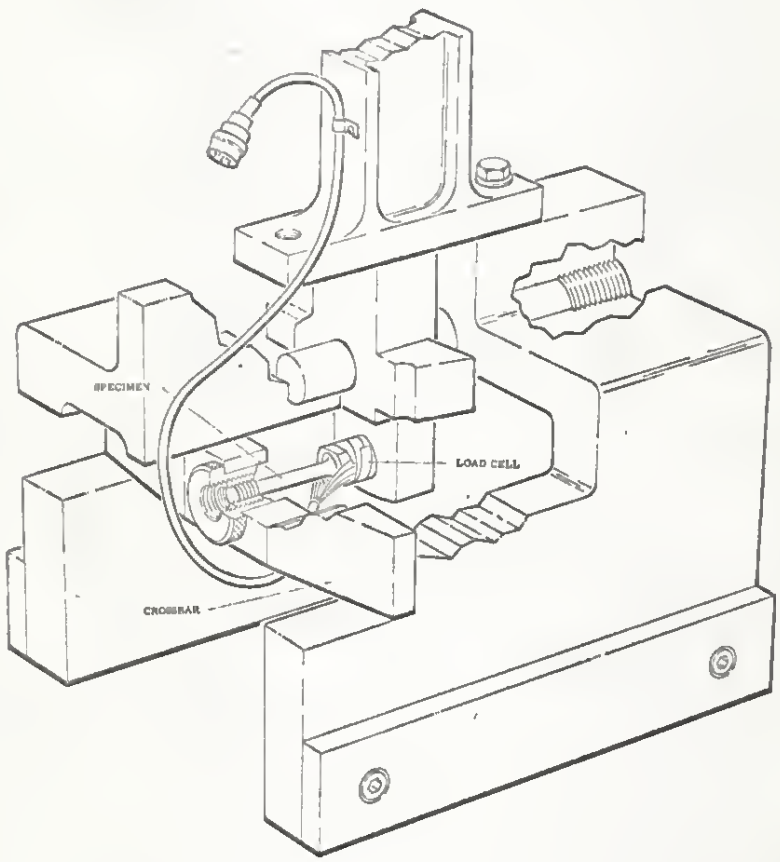

Fig. 8. Position of specimen, load cell, and crossbar pendulum head, Smith.

$\bar{F}_{k,k+1}$ is the average load during the interval t_k, t_{k+1}.

The pendulum linear velocity is given by

$$V_k = \left(\frac{2\,E_k'}{m}\right)^{1/2}$$

where m is the mass of pendulum referred to the center of percussion and the pendulum linear motion from t_o to t_k is given by

$$S_k = \sum_{0}^{k} V_k(t_{k+1} - t_k)$$

Applying this routine to the load-time record beginning at t_o with the known values of E_o and V_o results in a record of velocity and displacement as a function of time throughout the test. By taking 20 to 25 time divisions, calculated final velocity and final elongation were checked with measured elongation and velocity; an error of within ± 2 per cent was found. The calculated displacement was converted to engineering strain by using the formula

$$\epsilon = (S - a - bt)/L$$

where L is the original length of the specimen; a and b were calculated from the independently known values of time and strain at yield and fracture. Plot of strain versus time gives strain rate. Nominal strain rate was taken as V_o/L since the velocity change during the test was small.

Steidel and Mekerov also used a pendulum impact type testing machine as shown in Fig. 9. A high-speed Fastax camera was used to record photographically the elongation and the reduction of area during the impact.

True dynamic stress was computed by dividing the load by the true area of the specimen obtained from the high-speed camera records. The nominal stress was obtained by dividing the load by the nominal area of the specimen.

Strain could be obtained either by using reduction of area or by using elongation. The nominal strain rate was obtained from the gage length and specimen velocity by using the formula

$$\dot{\epsilon} = \frac{1}{L} \frac{d\ell}{dt}$$

where L is the gage length, and

$\frac{d\ell}{dt}$ is the corresponding velocity.

The true strain rate was measured as follows:

$$\dot{\epsilon} = \frac{2 \ell n \frac{D_1}{D_2}}{t_2 - t_1}$$

where D is the instantaneous diameter of the specimen as obtained from the high-speed camera records

t is the time obtained from the known velocity of the film per frame.

True strain rate can be obtained only when the necking of the specimen starts.

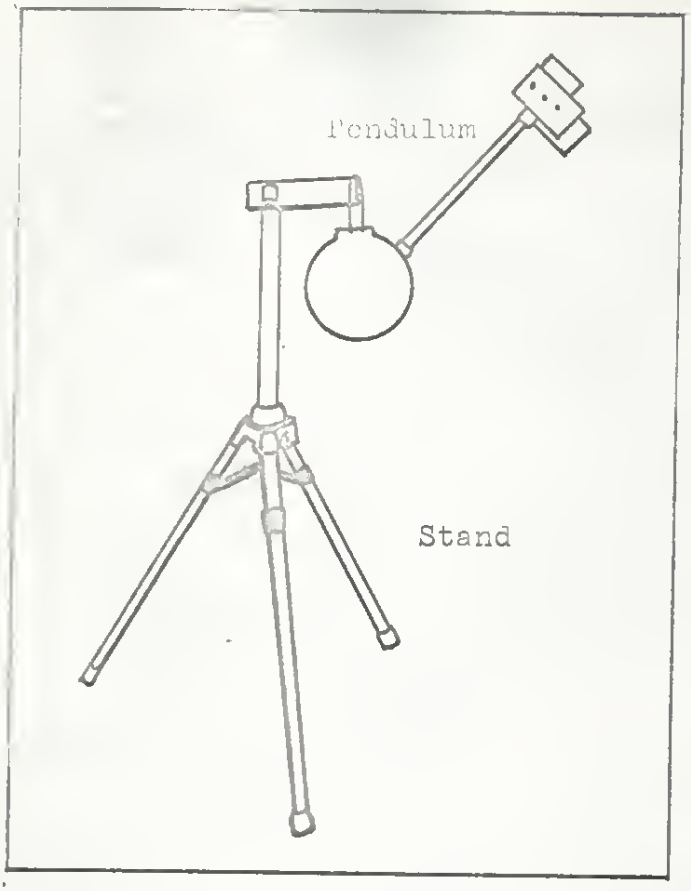

Fig. 9a. General view of the apparatus, Steidel and Makerov.

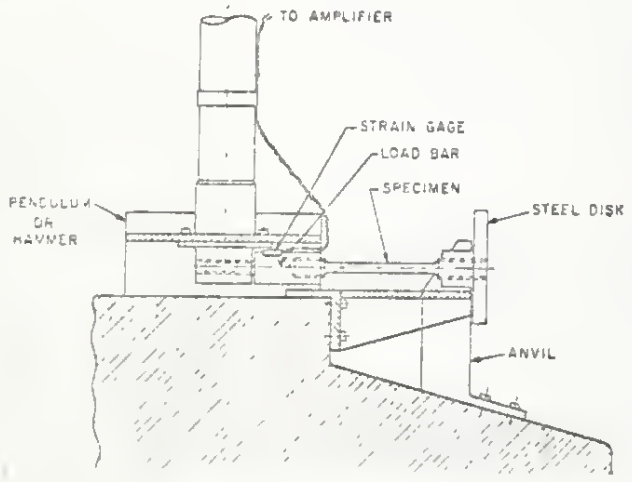

Fig. 9b. Arrangement of pendulum, anvil, and specimen, Steidel and Makerov.

Steidel and Austin used an explosively loaded tensile tester; the machine is shown in Fig. 10. A high-speed camera was used to record photographically the reduction of area and the impact velocity. Since the oscilloscope sweep was triggered externally when the piston contacted a pencil lead after some initial elongation of the specimen, the entire load-time curve was not obtained. Therefore linear extrapolation of the load curve was made to obtain values prior to necking. Because the duration of the flash lamp was only 200 microseconds, the flash lamp trigger was set to get pictures starting with the beginning of necking. The camera was operating during the entire ignition time, but the exposure of the film occurred only upon firing of the flash lamp. A standard one-inch length next to the specimen provided accurate calibration of each frame and compensated for any shrinkage or stretching of the film. Measurements of the piston displacement was provided by a 1/8-inch velocity rod which moves with the piston. The height of this rod above a fixed point on the cylinder block subtracted from the initial height, determined the piston displacement at each frame, and also provided measurement of impact velocity by extrapolation.

Stress, strain, and strain rate were calculated in the same way as by Steidel and Makerov. Even though the length of reduced area section was 1.25 inches, the calculations were based on a one-inch gage length.

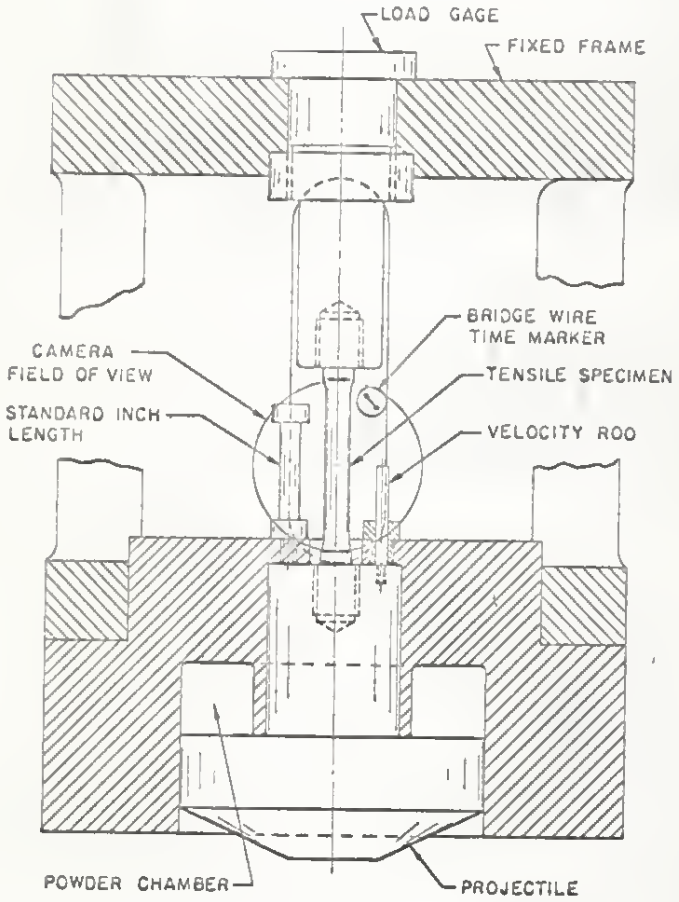

Fig. 10. Impact tensile tester camera field of view, Austin and Steidel.

Tubular Specimens

Kendall and Ginsburgh used the shock tube testing machine shown in Fig. 11; see Appendix II for details. Figure 12 shows the specimen used in the test. The pressure produced inside the test tube was measured by two pressure probes located in the shock tube, one at 2.5 feet and the other at 10 feet from the spark end. Usually several trials were run on each specimen, starting with a pressure which was expected to produce no yielding and increasing the pressure about 30 per cent each trial until the specimen burst.

The yield stress was calculated from the formula

$$\sigma_y = \frac{PR_o}{h}(1 - B) \quad \text{(Derived in Appendix II.)}$$

where R_o is the original inside radius and B is the negative root obtained from

$$B^2 - B\left(A \frac{2\,Eh}{PR_o^2}\right) - 1 = 0.$$

A = permanent change of tube radius.

Note that the value of B calculated by the equation is at the yield point only, but if A is known as a function of time, then B can also be calculated as a function of time. Therefore stress can also be calculated as a function of time. Measurement of permanent deformation was made by removing the shield after each shot and measuring the specimen diameter with a micrometer. The amount of plastic deformation in each shot was

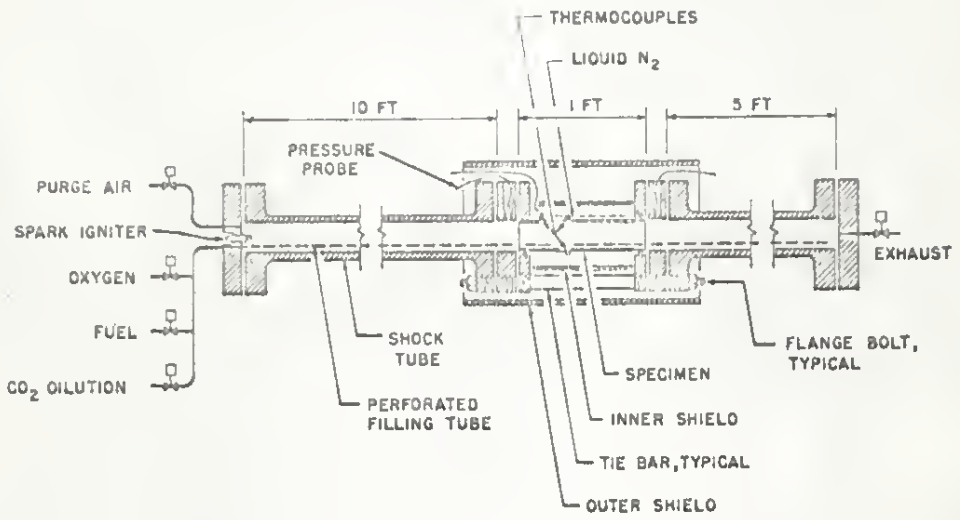

Fig. 11. Shock tube test equipment, Randall and Ginsburgh.

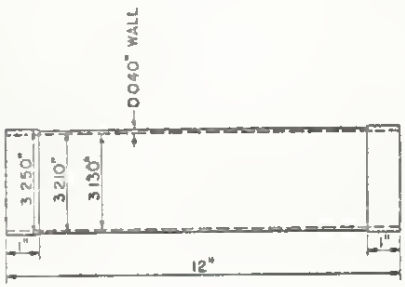

Fig. 12. Test specimen, Randall and Ginsburgh.

obtained by averaging the two measurements of the diameter, taken at right angles to each other, at the center of the specimen. Permanent deformation in the final shot (which caused bursting of the tube) was measured by the change in thickness of the wall. To convert the reduction of thickness to circumferential strain, it was assumed that the strain in the thickness direction was one-half the circumferential strain. The stress before yield could be calculated by using the value of B in terms of t, i.e.,

$$\sigma = \frac{PR_o}{h}\left[1 - \cos\frac{t}{R_o}\left(\frac{gE}{\rho}\right)^{1/2}\right].$$

The strain up to yielding could be calculated by dividing by E, i.e.,

$$\epsilon = \frac{PR_o}{Eh}\left[1 - \cos\frac{t}{R_o}\left(\frac{gE}{\rho}\right)^{1/2}\right].$$

The strain rate at the instant yielding began was obtained from the equation

$$\dot{\epsilon}_y = \frac{P}{Eh}\left(\frac{gE}{\rho}\right)^{1/2}(1 - B^2)^{1/2}$$

Clark and Duwez used the impact testing machine as shown in Figs. 13a and 13b. The specimen used by them is shown in Fig. 14. The hammer velocity was determined just before the impact. A dynamometer was used to obtain force as a function of time.

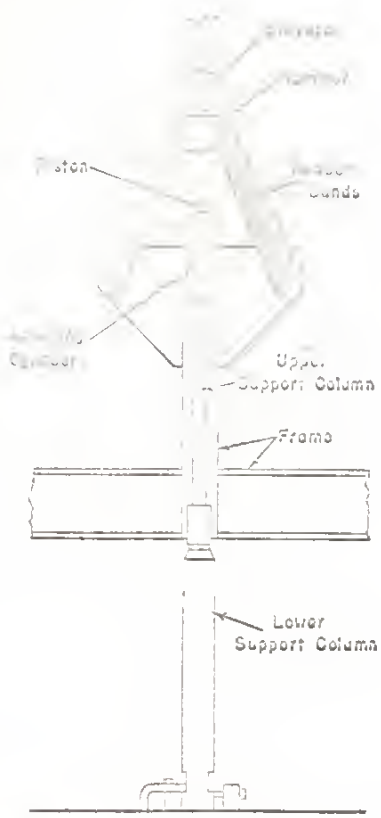

Fig. 13a. Strain rate machine, Clark and Duwez.

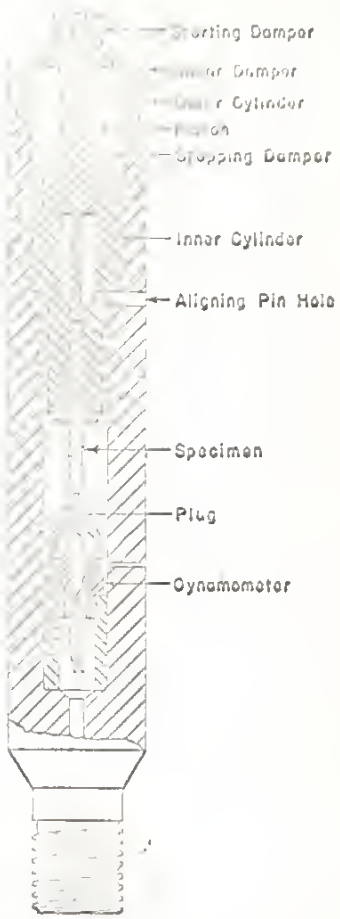

Fig. 13b. Actuating cylinder assembly, Clark and Duwez.

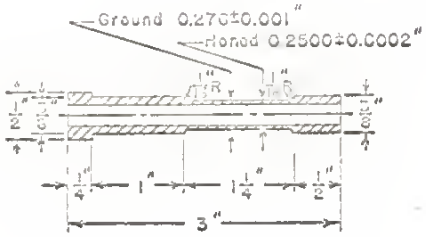

Fig. 14. Test specimen, Clark and Duwez.

The ultimate strength was computed by means of the formula

$$\sigma = \frac{PRa}{\rho} .$$

The average radius, Ra, of the cylinder was measured on that part of the ruptured cylinder which remained nearly cylindrical in shape and not in the region of the fracture.

The strain was calculated by using the initial and final diameters. Because mercury has a very low compressibility coefficient, about 4×10^{-6} atmospheres^{-1}, it was assumed to be incompressible. With this assumption, the strain rate was calculated from the formula

$$\frac{d\epsilon}{dt} = \left(\frac{R_p}{R}\right)^2 \frac{1}{2L} V_p$$

where p stands for piston.

Figure 15 shows the tube impact test figure used by Noyes. The specimen used for the experiment is shown in Fig. 16. The stresses were produced by a falling weight. For measuring pressure, a 1/4-inch diameter hard aluminum rod was used inside the specimen and coaxial with it. Two gages were mounted on this rod, being diametrically opposed and aligned so as to respond to hoop strains in the rod. The rod is a sliding fit both at its upstream and downstream ends. The hoop stress was calculated by using the inside diameter, R_o, of the original specimen from the formula,

$$\sigma = PR_o/h$$

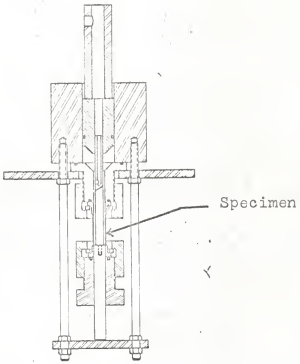

Fig. 15. Tube impact test fixture, Noyes.

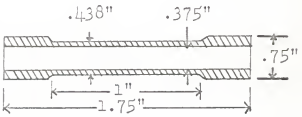

Fig. 16. Test specimen, Noyes.

The strain and strain rate were calculated by using one gage on the specimen as well as by measuring the uniform diameter of the ruptured specimen and the total time up to rupture. No information is available about where the gage was located on the specimen.

Hoge used the Dynapak testing machine (Fig. 17) with some modifications to perform tests on tubular specimens, Fig. 18. For measuring stresses, data were obtained from strain gages and also a pressure transducer. The tests indicated that a constant-stress field was produced at points from 1.5 to 3 inches from the lipped end of the specimen. The stresses calculated from strain gage readings in the region were within a few per cent of those calculated from the pressure transducer. The stresses were calculated from the formulas

(Hoop) $$\sigma_1 = \frac{P(R_o^2 + R_i^2)}{(R_o^2 - R_i^2)}$$

(Meridional) $$\sigma_2 = \frac{P\,R_i^2}{(R_o^2 - R_i^2)}$$

The strains were obtained from the strain gages mounted on the specimen as shown in Fig. 18. The strain rates were obtained from the slope of the strain-time curve.

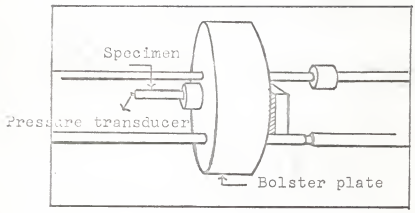

Fig. 17. Dynapak machine setup for tubular specimen, Hoge.

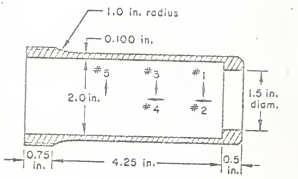

Fig. 18. Tubular specimen, Hoge.

RESULTS

Figure 19 shows the plot of the ratio of dynamic stress to static stress versus strain rate for 6061-T6 aluminum alloy. The results are taken from the works of Austin and Steidel, Steidel and Makerov, Hoge, and Smith.

The ratio of dynamic stress to static stress for copper is shown in Fig. 20. Shepler used pure copper, annealed at 350 C for 15 minutes and cooled to 75 C. The condition of copper used by Clark is unknown. Manjoine and Nadai used pure copper, heated to 500 C in 5 hours and cooled to room temperature in 12 hours. Copper used by Smith was hard tempered.

Figure 21 is the plot of the stress ratio as a function of strain rate for some steels obtained from the work of Clark. The types of steel used and SAE 1020 hot rolled, SAE 1035 annealed at 1550 F, SAE 1112 cold draw, free cutting steel, and SAE 6140 quenched in oil from 1575 F, tempered at 1020 F.

Results obtained from the work of Clark on SAE X4130 steel under different conditions are shown in Fig. 22 where stress ratio is plotted as a function of strain rate. The four different conditions of SAE X4130 steel were:

a. Annealed at 1575 F.

b. Quenched in oil from 1575 F, tempered at 1000 F.

c. Quenched in oil from 1575 F, tempered at 800 F.

d. Quenched in oil from 1575 F, tempered at 600 F.

Figure 23 is a plot of stress ratio as a function of strain rate for steel. Steidel and Makerov used cold rolled steel (type not known), Shepler used SAE 1020 CR steel,

annealed at 1500 F for two hours. Manjoine and Nadai used low carbon mild steel, annealed at 1688 F for one hour.

Because of the uncertainty of the data obtained from the [illegible], Noyes did not give any results. From the photographs of the fractured specimen, Noyes concluded that the amount of uniform deformation increased with increasing strain rate.

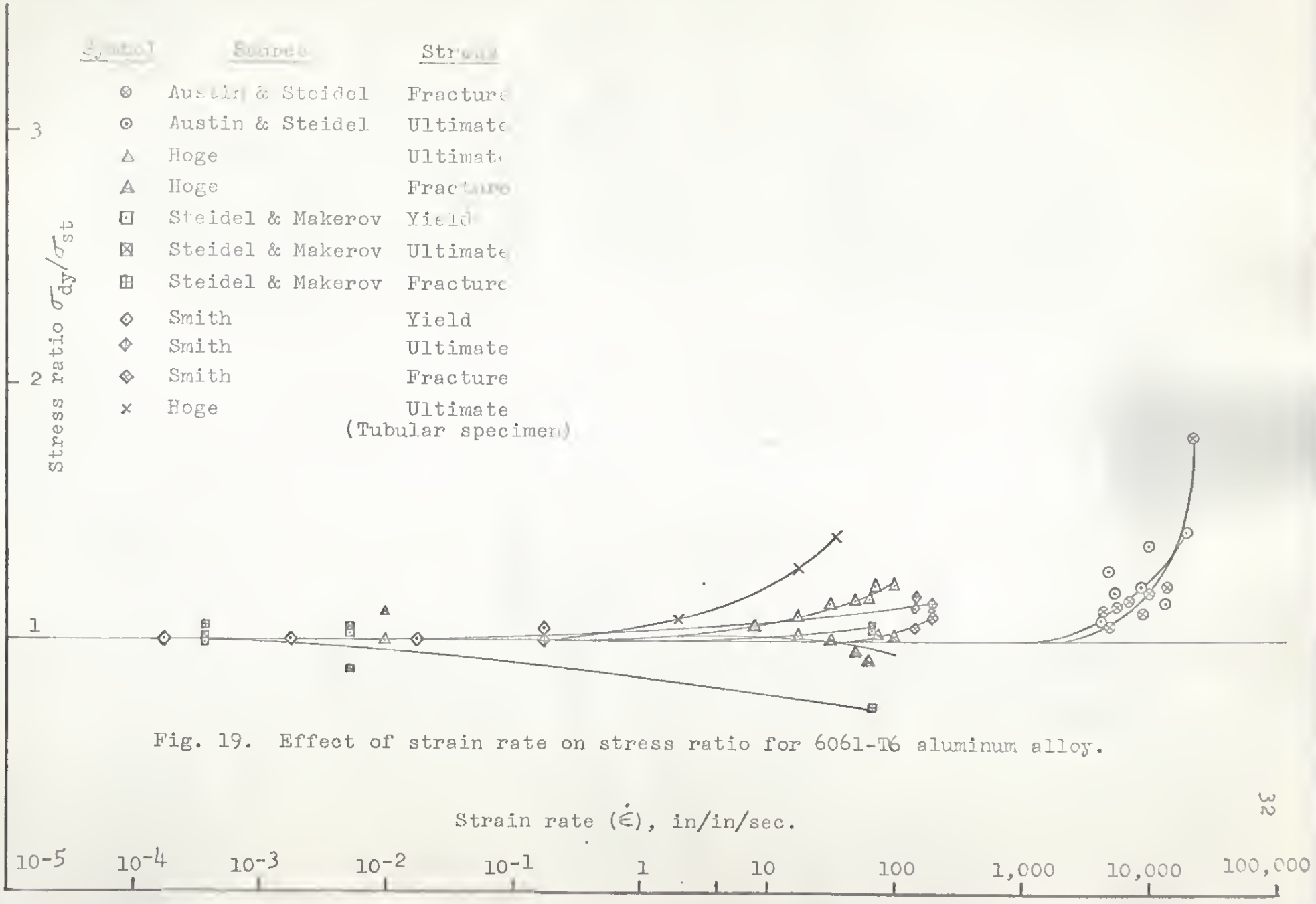

Fig. 19. Effect of strain rate on stress ratio for 6061-T6 aluminum alloy.

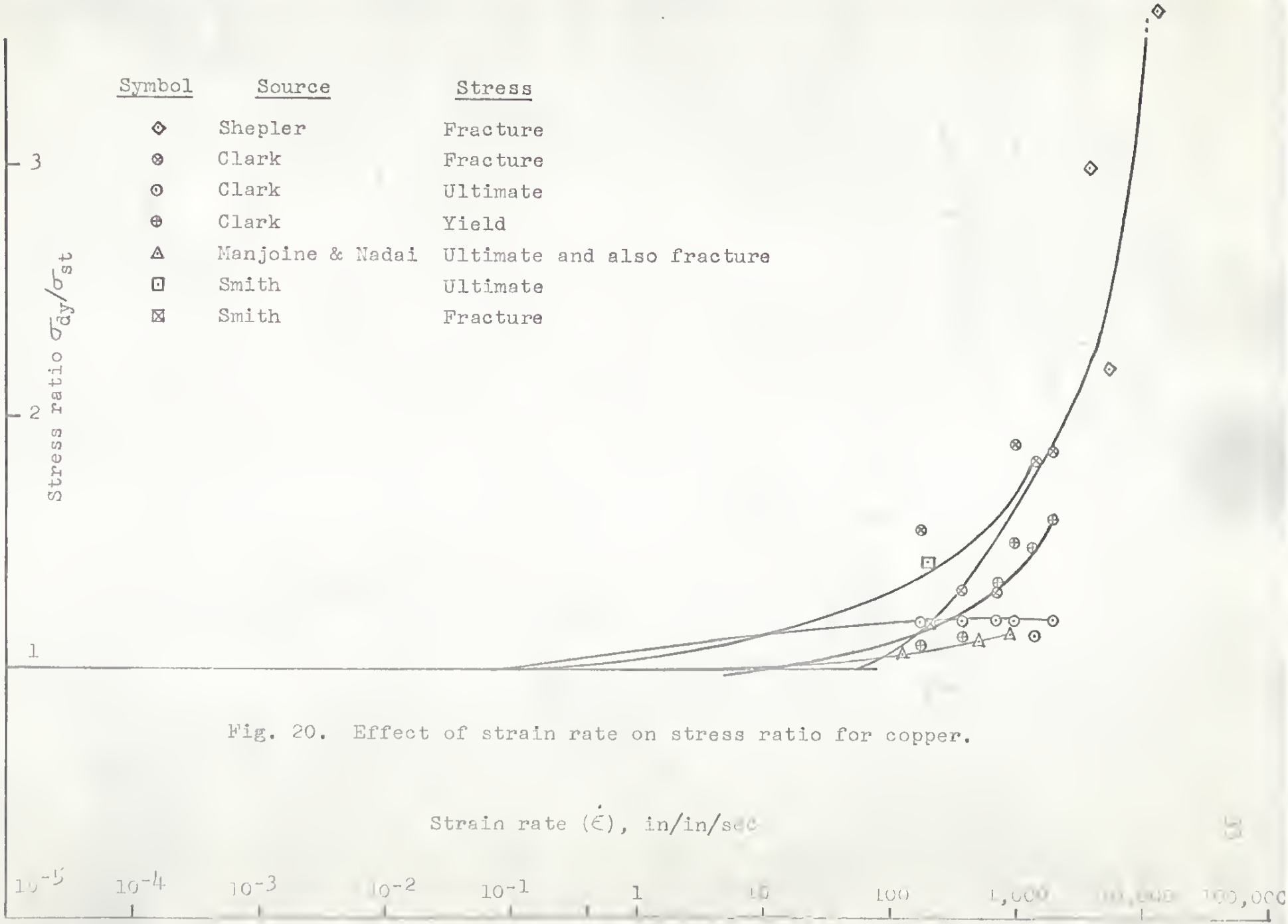

Fig. 20. Effect of strain rate on stress ratio for copper.

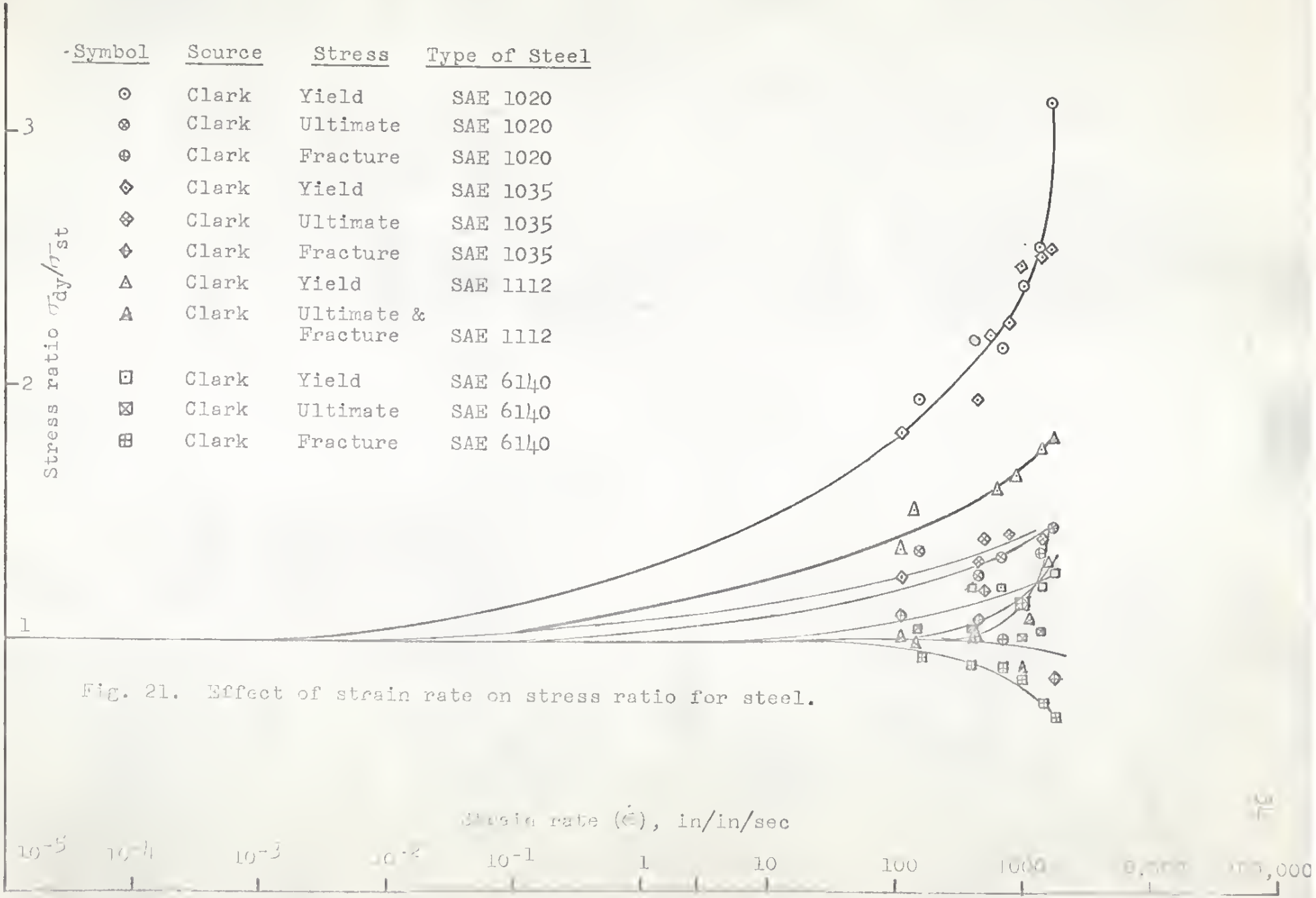

Fig. 21. Effect of strain rate on stress ratio for steel.

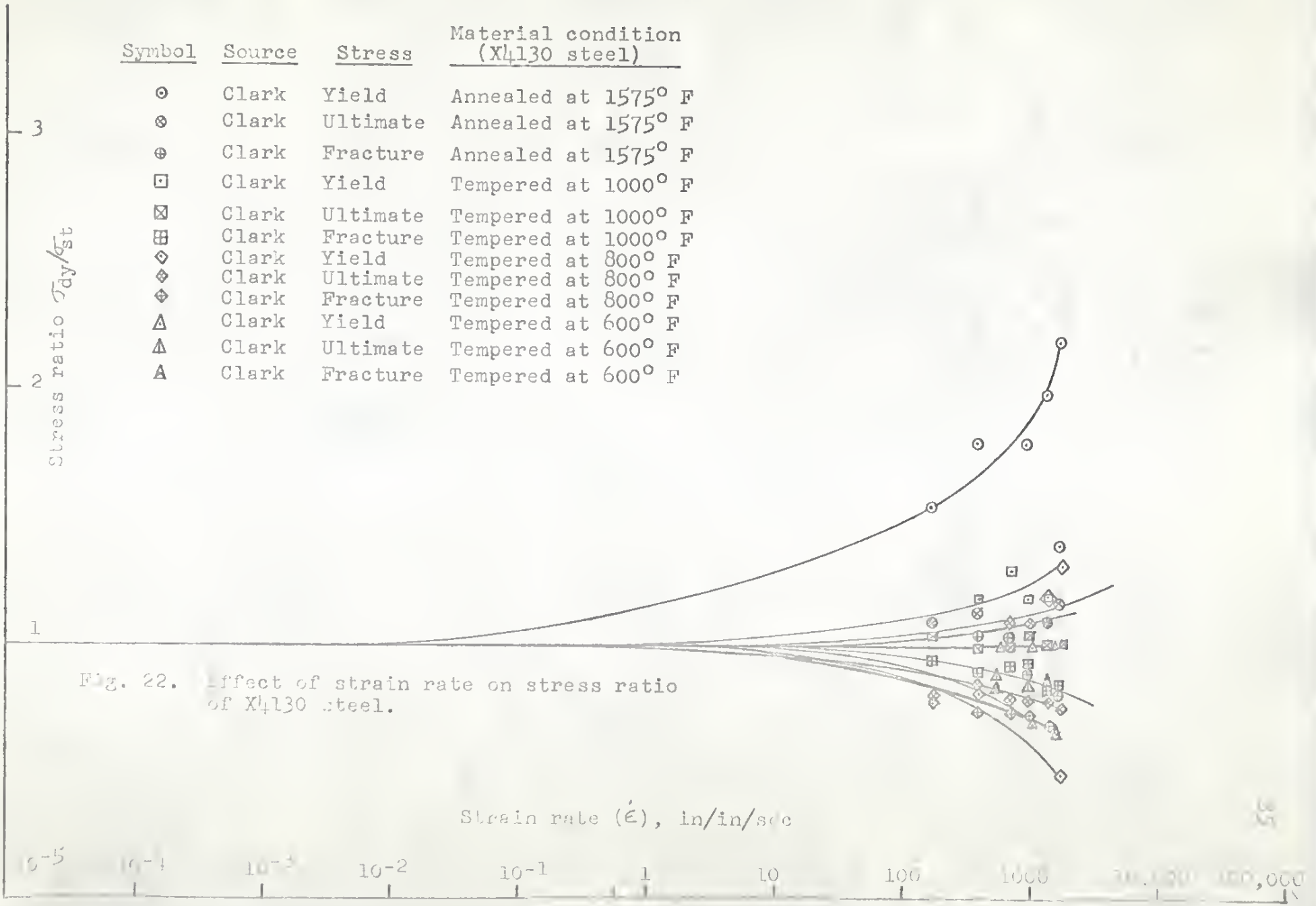

Fig. 22. Effect of strain rate on stress ratio of X4130 steel.

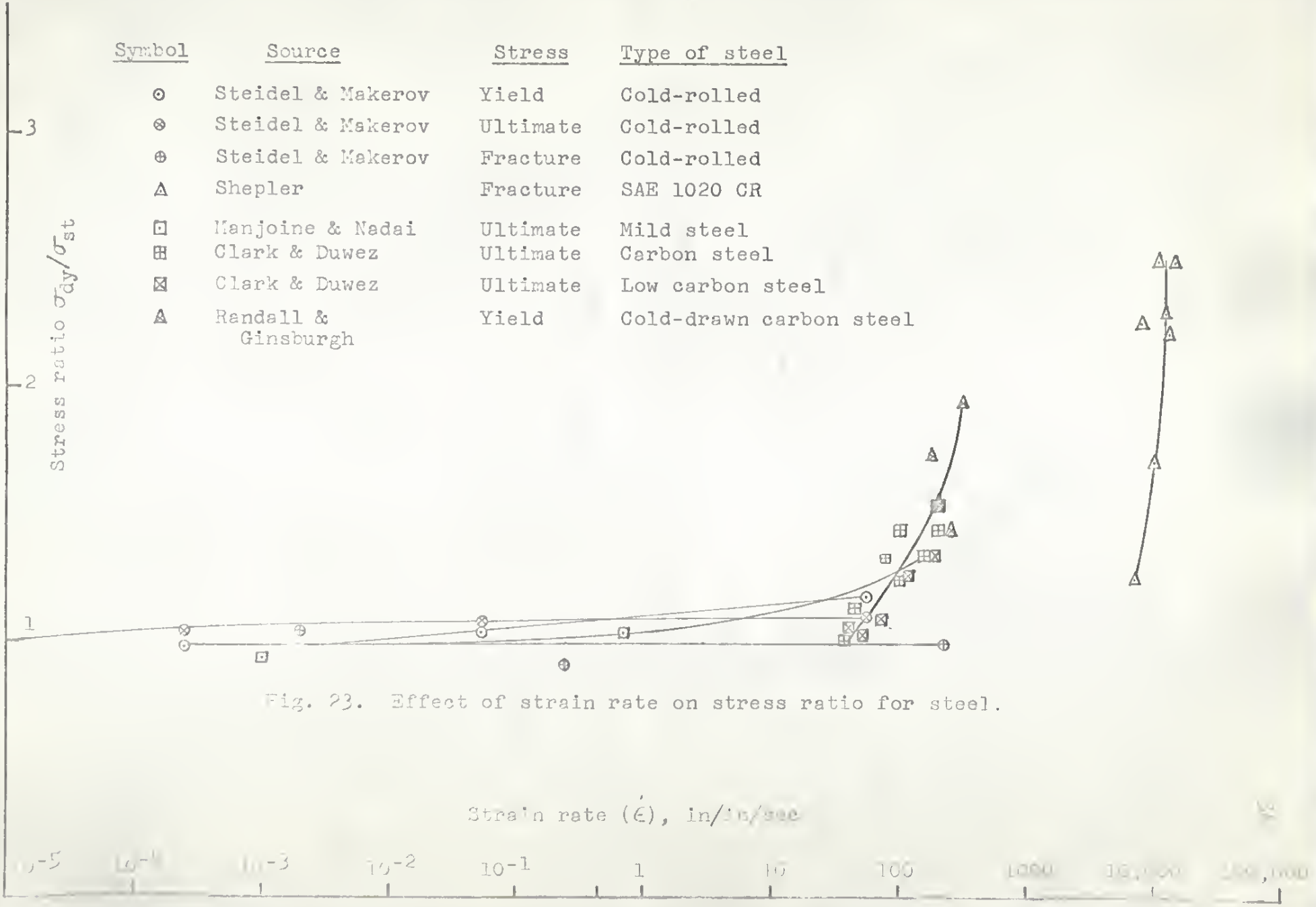

Fig. 23. Effect of strain rate on stress ratio for steel.

DISCUSSION

Figure 19 shows the plot of stress ratio (Dynamic/Static) as a function of strain rate for 6061-T6 aluminum. The strain rates calculated by Austin and Steidel were at the portion where necking took place and based on changes of diameter. Hoge calculated the strain rate using the increase in the total length of the specimen including threaded portion. If Hoge had measured strain rate at the necking section, either based on diameter change or a shorter axial gage length, the strain rate would have been much greater for the strength obtained. This would shift the curve for Hoge's data toward the right and it would agree better with the results of Austin and Steidel. The curves for ultimate strength obtained by Steidel and Makerov, and Smith agree well with each other; this is because Steidel and Makerov used change in diameter for the calculation of strain rate and Smith used a short axial gage length. Similarly, the curves for yield strength obtained by Smith and by Steidel and Makerov also coincide.

There seems to be no similarity between the curves for fracture strength. If Hoge had measured strain rate at the necked portion, either by using the change in diameter or a small axial gage length, higher strain rates would be obtained and the curve would be shifted towards the right; but if the curve obtained by Steidel and Makerov, which is based on the strain rate calculated by using the change in diameter, is extended towards higher strain rates, there will be a great

deviation between this and the curve obtained by Hoge. Note that both show a decreasing value of ratio with increase in strain rate, whereas the curves obtained from the work of Austin and Steidel, and of Smith, show an increase.

If the curve for Smith is extended, it does not seem to agree with that for Austin and Steidel. The reason might be that in almost all experiments it was difficult to measure, from the load-time record, the exact value of load at fracture because the fracture point was not well defined. The load-time curve dropped to zero in a curved form rather than a straight line, the latter will define the fracture point exactly. According to Austin and Steidel, the error in measuring load at fracture may be about 10 to 15 per cent. It is also found that sometimes the cross section after fracture does not remain circular; it rather takes an elliptical form. The strain rate calculated by using the major diameter may differ from that calculated by using the minor diameter by about 16 per cent.

Plot of stress versus strain rate for copper is shown in Fig. 20. If the curve for fracture ratio obtained by Clark is extended, it seems to join the curve of Shepler. Note that both of them used the total length of the specimen in calculating strain rates. The curves for ultimate strength obtained by Clark, and Manjoine and Nadai are also close to each other. This shows the agreement of the results obtained by Clark, Manjoine and Nadai, and Shepler. Because enough data were not available from the work of Smith, only two points, one for

ultimate strength ratio and the other for fracture ratio are available and shown in Fig. 17. Neither point agrees with the results of the other investigators.

Clark performed tests on different types of steel; the stress ratio versus strain rate is shown in Fig. 21. As the number of steel increases, e.g., 1020 to 1112, the stress ratio relatively decreases. The SAE 1020 and SAE 1035 steels have a common curve for ultimate strength ratio; similarly, a common curve for ultimate ratio and a common curve for fracture stress ratio. The curve for the yield of SAE 1112 is lower than that of SAE 1020 and SAE 1035, and the curve for the yield strength of SAE 6140 is lower than that of SAE 1112; similar relation is found for ultimate strength also. All the curves show an increase in stress ratio with strain rate, except the fracture stress ratio for SAE 1112 and SAE 6140 steel. In general, the stress ratio decreases as the number of steel increases from SAE 1020 to SAE 6140. It can also be said that SAE 1020 steel is stronger than higher or lower carbon content steels.

Figure 22 shows the effect of tempering on X4130 steel; the data are obtained from the work of Clark. The specimens tempered at 600 and 800 F show a decrease of ultimate strength with increase in strain rate, while those tempered at 1000 F show no change; the annealed specimens show an increase. The yield point of the specimens tempered at 600 F and 800 F decreases with increasing strain rate. This, coupled with the decrease of ultimate strength, is indicative of the poorer dynamic properties of this material when tempered at 600 and

500 F than when tempered at 1000 F. The yield strength of the annealed specimen increases rapidly compared to the others.

The stress ratio as a function of strain rate for steel is shown in Fig. 23. It is difficult to make any comparison with others because the type of steel used by different experimenters is not the same. Clark and Duwez, and Randall and Pinsburgh used carbon steel which might include the SAE numbers of the order of 10XX and 11XX. In Fig. 20, one curve is drawn through all the points obtained from their work, which shows the agreement of the results. It was noticed in Fig. 21 that the curve belonging to SAE 1020 steel shows higher stress ratio compared to others; a similar phenomenon is noticed in Fig. 23 also. Manjoine and Nadai used mild steel and Steidel and Makerov used cold rolled steel; note that both types of steel include a wide range of SAE numbers. Therefore no comparison of the test techniques is made.

In most of the experiments performed on the solid rod specimen, the strains were calculated from the total elongation or reduction in diameter obtained from post fracture measurement of the broken specimen. In some experiments, the strain rates were computed from a measurement of the total time, from yield to fracture. This kind of measurements does not give any idea about how the length or diameter is changing during the time from impact to fracture. The method of measuring strains and strain rates used by Austin and Steidel seems to be the best because in this a high-speed camera took pictures which show the exact change in diameter of the specimen with time.

CONCLUSION

In general, two types of techniques were used in measuring strain rates; one was on the elongation of the total length of the specimen and the other on a small axial gage length or change in diameter at the necking portion. If all the results were compared by converting them to look as if they were based on change in the diameter or small axial gage length, there seems to be a better agreement of the results. Mostly, the results disagree with each other at fracture. The reason may be the difficulty in reading the exact value of load at fracture from the load-time record. Another difficulty was that in some cases the fractured cross section was elliptical rather than circular; an error can be expected between the strain rates calculated by using the major or minor diameter of the elliptical section.

Some experimentera used photoelectric cells or an accelerometer to obtain elongation in the length of the specimen as a function of time, but there was no arrangement for measuring change in diameter as a function of time. One method of measuring diameter as a function of time might be to use some kind of arrangement involving photoelectric cells.

Acknowledgment

The author wishes to thank Dr. John D. Dingholm, Major Professor, for his advice and counsel during the preparation of this report.

BIBLIOGRAPHY

1. Shapley, P. R.
Explosive impact tests. Proc. of the SESA, Vol. 5, No. 1, 1947.

2. Hoge, K. G.
Influence of strain rate on mechanical properties of 6061-T6, aluminum under uniaxial and biaxial states of stress. Experimental Mechanics 2, 1965.

3. Anderson, A. G. H.
A medium speed tensile testing machine and some dynamic data produced thereby. High Speed Testing, Vol. IV, 1963.

4. Clark, D. S.
The influence of impact velocity on the tensile characteristics of some aircraft metals and alloys. NACA Technical Note 866, Oct., 1942.

5. Manjoine, M. and A. Nadai.
High-speed tension tests at elevated temperatures. Proc. of ASTM, Vol. 40, 1940.

6. Smith, J. E.
Tension tests of metals at strain rates up to 200 sec^{-1}. Materials, Research, and Standards, Vol. 3, 1963.

7. Steidel, R. F. and C. E. Makerov.
The tensile properties of engineering materials at moderate rates of strain. ASTM Bulletin No. 243-250, 1960.

8. Austin, A. L. and R. F. Steidel, Jr.
A method for determining the tensile properties of metals at high rates of strain. Proc. of SESA, Vol. XVII, No. 1, 1959.

9. Randall, P. N. and I. Ginsburgh.
Bursting of tubular specimens by gaseous detonation. Journal of Basic Engineering, Vol. 82-83, 1960-1961.

10. Clark, D. S. and P. E. Duwez.
The influence of strain rate on some tensile properties of steel. Proc. ASTM, Vol. 50, 1950.

11. Nevis, R. B.
Rapid bursting of tubular specimens. High-speed Testing. Vol. IV, 1963.

12. Den Hartog, J. P.
Advanced strength of materials. New York: McGraw-Hill Book Company, 1952.

APPENDICES

APPENDIX I

Shepler Tester

Figure 2 shows a view of the tensile machine used by Shepler. One end of the specimen is connected through the load gage to the fixed rear nut. The front end of the specimen is connected to the front nut which carries an accelerometer. The powder chamber is filled with the desired amount of explosive powder. When powder is burnt, it pushes the piston rapidly in a forward direction causing tension in the specimen. By changing the weight of the moving part and also by changing the volume of the powder chamber, the rates of strain can be changed.

Hoge Tester

Hoge used the 600 Dynapak tensile machine which is shown in Fig. 3. In this machine, nitrogen, stored at pressures up to 2000 p.s.i., is allowed to expand rapidly against a 6-inch piston, driving it and a ram at high velocity. The ram impacts the ram plate, moving it and the reverse tension plate at correspondingly high velocities. The ram plate and the reverse tension plate are connected by these shafts which slide through rulon bushings in the bolster plate. One end of the specimen is connected to the bolster plate through the load cell, whereas the other end is connected to the reverse tension plate. The bolster plate is fixed and has the ability to quickly stop the ram and absorb its energy. The velocity and net forces acting

can be adjusted by setting various combinations of fire pressure, ram weight, and distance between the ram and ram plate.

Anderson Tester

Figure 5 shows the tensile tester used by Anderson. High pressure nitrogen is allowed to enter into the cylinder through the poppet valve. This high pressure gas moves the piston upwards with high velocity. The upper end of the piston is connected to the yoke which also moves with the piston. The upper end of the specimen is connected to the upper end of the yoke through the load transducer, whereas the lower end is connected to the fixed frame. Piston speed can be adjusted by adjusting the pressure of nitrogen as well as by changing the weight of the piston.

Clark Tester

Figure 6 shows the impact machine used by Clark. Rotating disc, A, has striking jaws, B, connected to the periphery. One end of the specimen is screwed into the dynamometer, E, which is fixed at the end of an anvil, F. The anvil is fixed to the base. The other end of the specimen is screwed into a tup, M, consisting of a piece of steel one inch square and one-half inch thick. After the wheel reaches the desired speed, the striking jaws are extended and engage with the tup loading the specimen in tension. The rate of strain can be changed by changing the speed of the rotating disc.

The constancy of the wheel velocity during impact was checked by an extensometer P. It consists of a small cylinder one-fourth inch in diameter and one inch long, mounted at the end of the dynamometer, parallel, and above the specimen gage length as in Fig. 6. This cylinder consists of 115 alternate layers of 0.009-inch celluloid and 0.001-inch aluminum foil pressed on to a central steel shaft in such a manner that the aluminum discs make electrical contact with the central shaft. The outer surface of the cylinder is smooth. A narrow ribbon of clock spring steel, carrying a needle point at one end, is fastened to the tup prior to fracture of the specimen. This ribbon is held along an element of the cylinder by an elastic rubber tube. As the tup is drawn forward during deformation of the specimen, the needle point scratches the surface of the cylinder, alternately making and breaking an electrical circuit after every 0.01 inch of elongation. This produces successive modulates on the force-time diagram corresponding to deformation units of 0.01 inch. Because equal units of elongation were marked at equal time intervals, it was concluded that the velocity of the wheel during fracture was essentially constant.

Manjoine and Nadai Tester

Manjoine and Nadai used a rotating disc type impact machine, Fig. 7. The machine consists of a flywheel, g, driven by a direct-current motor, a pair of hammers, f, rotating with the wheel, and a pair of vertical columns carrying a heavy cross piece on which the test specimen is mounted in a vertical

position. The force measuring bar is attached to the upper crosshead, k. The specimen, c, carries at its lower end an anvil, d, a short cross piece of steel which is threaded to admit the test bar. When the trigger, h, is released the hammers are rotated to their striking position by means of spring, j, attached to the flywheel. The tensile force is applied to the specimen when the hammers strike the anvil. By adjusting the speed of the rotating wheel, different rates of strain can be obtained.

Smith Tester

Smith used a pendulum type impact machine as shown in Fig. 8. This figure shows the position of specimen, load cell, and crossbar within the pendulum head. In operation, the pendulum is raised to a position to deliver desired velocity and energy. Just before impact of the crossbar and anvil, the pendulum head contacts a trigger pin, starting the oscilloscope sweep. The crossbar is then stopped by the anvil, loading the specimen in tension as the pendulum continues its swing. The strain rate can be varied by varying the height to which the pendulum head is taken before releasing.

Steidel and Makerov Tester

Figure 9a shows the pendulum type impact machine used by Steidel and Makerov. The test specimen was fixed to the pendulum. A striking disc was fixed at the other end of the specimen. Figure 9b shows the detailed view of the specimen at the

time of impact. When the pendulum is released from a certain height, it takes a swing, the steel disc strikes the anvil causing tension or rupture of the specimen. The high-speed camera had a speed of about 7000 frames per second. Floodlights were used to illuminate the specimen. Different strain rates can be obtained by varying the height of the pendulum head before releasing.

Steidel and Austin Tester

Figure 10 shows the explosive impact testing machine used by Steidel and Austin. The upper end of the specimen is connected to the fixed frame through the load cell, the lower end is connected to the piston. The powder chamber is filled with desired amount of explosive powder. When the powder is fired, the piston moves downward at a high velocity; this causes tension in the specimen. A model 602 high-speed framing camera developed by Los Alamos Scientific Laboratory was used. The speed was 3,000,000 frames (1.2 cm x 1.4 cm) per second. The rate of strain can be varied by varying the weight of the piston as well as the amount of powder.

APPENDIX II

Figure 11 shows the shock-tube test equipment used by Randall and Ginsburgh. One shock tube was 10 feet long and the other was 5 feet long. Fuel and oxygen were supplied to the shock tube through a tube lying at the bottom of the shock tube (shown by dotted line in the figure). After thorough mixing of fuel and oxygen, the mixture was ignited. The detonation velocity and wave form are such that the effect on the tube may be treated as a suddenly applied pressure, uniform along the length of the tube. The ends of the specimen were sealed to the flanges by rubber O-rings such that they did not exert an axial thrust on the specimen. A stainless steel pipe of 1/4-inch wall thickness, lined with 1/2-inch thick sponge rubber (marked as inner shield in Fig. 11) was surrounding the specimen with some radial gap between the two tubes. This rubber embedded and retained the specimen fragments in their correct relative position after the bursting of the tube. The peak mixture in the tube can be varied by changing the amount of mixture.

Derivation of the Formulae
(Randall and Ginsburgh)

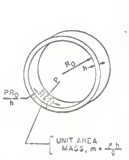

Referring to the above figure, the general equation of motion is that of a mass, the mass of a unit area of the pipe wall, acted upon by a suddenly applied force P, the pressure pulse, and by a restraining spring force, which is the radial component of the hoop stress in a unit length of the pipe wall. The hoop stress is given by

$$\sigma_t = \frac{PR_o}{h} .$$

If no longitudinal stress occurs, the hoop strain will be

$$\epsilon_t = \frac{r}{R_o} = \frac{\sigma_t}{E}$$

where r = increase in radius.

Therefore $$r = \frac{PR_o^2}{Eh} .$$

The pipe wall acts as a spring of stiffness K given by

$$K = \frac{P}{r} = \frac{Eh}{R_o^2} .$$

Note that the calculations are based on the mass m = eh/g of a unit area (as shown in the above figure).

Within the elastic region, the governing equation of motion for the pipe wall is obtained as follows. The wall is acted upon by two equal and opposite forces, namely, the spring force which is equal to the product Kr, and the force being that of

the pressure pulse. Thus according to D'Alembert's principle,

$$\frac{d^2r}{dt^2} = \left(\frac{P}{m}\right) - \left(\frac{Kr}{m}\right)$$

or

$$\frac{d^2r}{dt^2} + \left(\frac{K}{m}\right)r - \frac{P}{m} = 0 \ .$$

The solution of this equation is given by

$$r = rc + rp \ .$$

Let rp = A. Substitution of this in the equation of motion gives

$$0 + \frac{K}{m} A - \frac{P}{m} = 0$$

$$A = P/K$$

$$rp = P/K$$

Let $$r_c = B \cos\sqrt{\frac{K}{m}}\, t + C \sin\sqrt{\frac{K}{m}}\, t$$

Hence the solution of the equation of motion will be

$$r = B \cos\sqrt{\frac{K}{m}}\, t + C \sin\sqrt{\frac{K}{m}}\, t + \frac{P}{K}$$

At t = 0, r = 0

$$0 = B(1) + C(0) + P/K$$

$$B = - P/K \ .$$

Differentiating r with respect to time,

$$\frac{dr}{dt} = -B\sqrt{\frac{K}{m}}\sin\sqrt{\frac{K}{m}}\,t + C\sqrt{\frac{K}{m}}\cos\sqrt{\frac{K}{m}}\,t$$

At t = 0, dr/dt = 0

$$0 = -B\sqrt{\frac{K}{m}}(0) + C\sqrt{\frac{K}{m}}(1)$$

$$C = 0$$

Hence $$r = \frac{P}{K}\left[1 - \cos\sqrt{\frac{K}{m}}\,t\right]$$

or $$r = \frac{PR_o^2}{Eh}\left[1 - \cos\frac{t}{R_o}\left(\frac{gE}{\rho}\right)^{1/2}\right].$$

The circumferential strain will be radial motion divided by R_o. The circumferential stress is obtained by multiplying the strain by E, i.e.,

$$\sigma = \frac{PR_o}{h}\left[1 - \cos\frac{t}{R_o}\left(\frac{gE}{\rho}\right)^{1/2}\right].$$

The time, t_y, until the yielding begins, is given by

$$\cos\frac{t_y}{R_o}\left(\frac{gE}{\rho}\right)^{1/2} = 1 - \frac{\sigma_y h}{PR_o} = B\ .$$

From the trigonometric relations,

$$\sin \frac{\pi}{2} \left(\frac{P}{P_o}\right)^{1/2} = (1 - B^2)^{1/2}$$

Hence velocity and acceleration at the instant yielding begins are given by

$$\left(\frac{dr}{dt}\right)_y = \frac{PR_o}{Eh} \left(\frac{gE}{\rho}\right)^{1/2} (1 - B^2)^{1/2}$$

and

$$\left(\frac{d^2r}{dt^2}\right)_y = \frac{Pg}{\rho h} B \ .$$

The time elapsed from the initiation of yielding until the pipe wall is brought to rest is

$$\frac{\left(\frac{dr}{dt}\right)_y}{\left(\frac{d^2r}{dt^2}\right)_y}$$

Therefore the plastic extension A of the radius, which can be measured from the burst tube, is

$$A = \frac{1}{2} \left(\frac{dr}{dt}\right)_y^2 \Big/ \left(\frac{d^2r}{dt^2}\right)_y$$

or

$$A = \frac{PR_o^2}{2\ Eh} \ \frac{(B^2 - 1)}{B}$$

or

$$B^2 - BA \frac{2\ Eh}{PR_o^2} - 1 = 0 \ .$$

In the above equation, all the values are known except B; therefore B can be calculated knowing $\dot{\epsilon}_0$, the yield stress σ_y can be calculated. The strain rate at the instant yielding began was obtained by dividing the expression for velocity by $\dot{\epsilon}_0$, i.e.,

$$\dot{\epsilon}_y = \frac{V}{Eh} \left(\frac{\sigma_y}{\rho}\right)^{1/2} (1 - B^2)^{1/2}$$

Clark and Duwez Tests

Clark and Duwez used the strain rate machine as shown in Figs. 13a and 13b. In this machine, an impacting hammer slides between the two vertical rails and is accelerated by 40 rubber bands 3/8 by 1 inch. The hammer is lifted to the desired position and then released. This way it is brought to a desired velocity at impact. The piston velocity is taken to be the same as the hammer velocity just before impact. The hammer velocity is determined by measuring the time required for the hammer to travel between fixed points of known spacing placed on the frame of the machine near the point of impact. A free-fitting plug closes the lower end of the specimen and rests on a dynamometer; from the dynamometer a force time curve is obtained. The peak pressure in the mercury can be changed by changing the height of the hammer along the rails.

Noyes Tester

The tube impact test fixture used by Noyes is shown in Fig. 15. The method of applying pressure is the same as that used by Clark and Duwez. A hammer is lifted to certain position and then released. The hammer drives the piston which loads the specimen by a pulse of internal pressure. The specimen is fixed in such a way that no axial stresses will be created in the specimen due to the pressure pulse. The peak pressure in the fluid (SAE 60 oil) can be varied by varying the height of the hammer.

Hoge Tester

Figure 17 shows the Dynapak machine used by Hoge with some modification. This is the same as the one he used for impact loading of solid bar-type specimens. The specimen was fixed to the bolster plate by screwing it into the specimen holder. The other end was sealed by a disc pressing an O-ring against the protruding tip of the specimen. A piston with a cup seal compressed the fluid against the disc. The piston shaft slid through a rulon bushing in the bolster plate and was threaded into the ram plate. As in uniaxial tests, the ram impacted the ram plate which loaded the specimen.

AN EVALUATION OF ITS MEASURING TECHNIQUES USED IN HIGH STRAIN RATE TESTING OF MATERIALS

by

SAYEEDUDDIN SYED

M. Sc., Osmania University, 1964
B. S., Kansas State University, 1966

AN ABSTRACT OF A MASTER'S REPORT

submitted in partial fulfillment of the

requirements for the degree

MASTER OF SCIENCE

Department of Mechanical Engineering

KANSAS STATE UNIVERSITY
Manhattan, Kansas

1968

This report consists of an evaluation of measuring techniques used by different investigators in finding out the variation of the strength of the materials with rate of strain. The specimens used in these experiments were of two types--solid-rod type specimen and tubular specimen. The high-speed loading tests performed on solid-rod type specimens were of two types, explosive loading type and impact loading type. For impact loading, either rotating discs or falling pendulum type of equipments were used. In some experiments the rates of strain were calculated from the initial and final conditions of the specimen, and in others high-speed camera or photoelectric cells were used. In most of the experiments performed on tubular specimens, the specimen was filled with some fluid which was compressed either by falling weight or by explosive loading type machine. The high rates of strain in the tubular specimen were also obtained by the detonation of gaseous fuel and oxygen in the tube.

The materials used in these tests were aluminum, copper, and steel. The rates of strain were calculated either by measuring the elongation of the total length of the specimen or by measuring the reduction of the diameter at the necking portion of the specimen. For comparison of the test results, all the measuring techniques could be reduced to one standard way of measurement. In some experiments, if the strength is obtained for a particular strain rate which was measured by using the elongation of the total length of the specimen, then the same strength will be obtained if strain rate measurements were

based on the reduction in diameter at the necking portion. This kind of comparison of the results showed that they agree with each other as far as the ultimate strength and the yield strength are concerned; but there seems to be no agreement between the results for fracture stress. In general, the strength of the materials is seen to increase with increase in strain rate.